Journal of Oceanology and Limnology
Vol. 38 No. 6, P. 1746-1754, 2020
https://doi.org/10.1007/s00343-019-9218-2

Changes of marine productivity and sedimentary environment recorded by biogenic components in the Antarctica Ross Sea since the last deglaciation*

XIU Chun[1, 2, **], DU Ming[1], ZHANG Xu[2], HUO Suxia[1]

[1] *North China Sea Environmental Monitoring Center of Ministry of Natural Resources, Qingdao 266033, China*
[2] *East Sea Marine Environmental Investigating and Surveying Center of Ministry of Natural Resources, Shanghai 200137, China*

Received Aug. 29, 2019; accepted in principle Oct. 8, 2019; accepted for publication Nov. 18, 2019

Abstract Changes in the marine productivity and sedimentary environment since the last deglaciation in the Ross Sea are presented in this paper. Opal has replaced calcium carbonate as the major biogenic component and has a significantly positive correlation with total organic carbon (TOC), which indicates that siliceous phytoplankton controlled the absorption and release of carbon by the biological pump and was the main producer of marine organic matter. Using the AMS ^{14}C age framework, foraminiferal fossils and redox sensitive elements (RSEs), we found that both the sedimentary environment and marine productivity changed clearly in ~11 cal ka BP, which is more likely related with the melting and retreat of the Ross Ice Shelf. In addition, the increase of marine productivity promoted the sinking of more organic-matter to the seabed. A large proportion of oxygen in the bottom water body was consumed and more carbon dioxide was produced during the decomposition of organic matter, making the bottom water body more soluble to calcium carbonate.

Keyword: biogenic components; marine productivity; redox environment; ice shelf retreat; the Ross Sea

1 INTRODUCTION

The Southern Ocean, accounting for nearly 20% of the world ocean, has high primary productivity (Hiscock et al., 2003; Graham et al., 2015). It is also one of major sinks of atmospheric carbon dioxide (Gao et al., 2001), and plays an important role in the global carbon cycle and climate regulation. Located in the Pacific sector of the Antarctic Ocean (Fig.1), the Ross Sea covers an area of about 9.6×10^5 km^2, with a water depth between 200 and 1 000 m. It is bounded by Marie Byrd Land to the east, Victoria Land to the west, and the Ross Ice Shelf to the south. During the last glacial maximum, an expanded grounded ice shelf occupied the Ross Sea Embayment (Anderson et al., 2014). Regional differences appeared in the retreat of ice shelf. Ship et al. (1999) believed that the retreat of ice shelf occurred first in the western Ross Sea, such as JOIDES Trough and Drygalski Trough, then in the central and eastern Ross Sea. The Ross Sea Ice Shelf continued to collapse in the Holocene and finally stabilized. Based on Deep Sea Drilling Project (DSDP) and geophysical data, sedimentary basins in the Ross Sea were divided into the Victoria Land Basin, Central Trough, and Eastern Basin (Davey et al., 1982). The overlying sediments of >1 000 m thick are good media for studying the evolution of paleoceanographic productivity and sedimentary environment.

Marine primary productivity can be defined as the mass of organic carbon converted from inorganic carbon by plankton within unit time and unit area in the upper ocean (Barnola et al., 1987; Raynaud et al., 1992). Studies of marine productivity contribute to further understanding of global carbon cycles, the marine environment, and atmospheric composition

* Supported by the Public Science and Technology Research Funds Projects of Ocean (No. 201105003-2) and the Chinese Polar Environment Comprehensive Investigation & Assessment Programs (No. CHINARE2016-01-02)
** Corresponding author: oucgeology@163.com

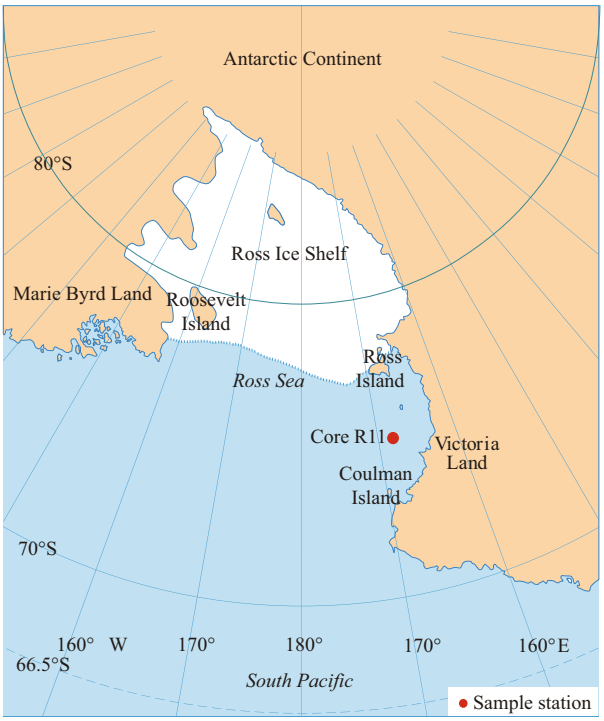

Fig.1 Regional unit of the Ross Sea

(Paytan et al., 1996; Bentaleb and Fontugne, 1998; Lin et al., 1999); however, supportive evidence from effective alternative indicators is needed, such as preserved organic carbon, biogenic calcium carbonate, and biogenic silica (Li et al., 2008; Liu et al., 2011). Biogeochemistry and primary productivity of the upper waters around the Antarctic Peninsula and in the Prydz Bay were discussed previously (Bonn et al., 1998; Fagel et al., 2002; Hu et al., 2007; Tan et al., 2014), but those in the Ross Sea were rarely involved. Moreover, due to lack of stratigraphic dating, marine productivity in the geological history remains poorly understood. In this paper, changes in marine productivity and the sedimentary environment since the last deglaciation are studied using the contents of biogenic components, a chronostratigraphic framework is established by combining data from foraminiferal fossils and redox sensitive elements (RSEs).

2 MATERIAL AND METHOD

2.1 Material

Core R11 was drilled and samples collected in the Ross Sea during the 31st China Antarctic Scientific Expedition at 167.81°E/74.95°S, in water depth of 448 m, and core length was 86 cm (Fig.1). The core was sectioned at 2-cm intervals, and the thickness of each sample was 2 cm; 22 samples were obtained.

According to the Folk's sediment classification (Folk et al., 1970), the majority of 22 samples were sandy silt, a few were silt, and only one sample was silty sand (Fig.2a). The sand proportion of the core at the depth of 68–84 cm reached 42.1% on average (Fig.2b), but dropped to 13.0% at core depths of 0–68 cm. Correspondingly, the mean of silt and clay increased from 57.9% to 87.0% over these same depth intervals. These data indicated that hydrodynamic conditions had changed significantly at the depth of 68 cm.

2.2 Method

The samples were ground after dried at 60°C. Dilute hydrochloric acid was added to the samples to remove inorganic carbon. After the reaction, high purity water was used to rinse the samples repeatedly until the pH was neutral. Fifteen milligram of each dried sample was wrapped in a tin cup, and analyzed for total organic carbon (TOC) and total nitrogen (TN) using a Vario Cube elemental analyser (Elementar UK Ltd.). The relative standard deviation (RSD) was less than 1%.

Opal content was measured using silicon-molybdenum blue colorimetry. A sodium carbonate solution was used to extract the biogenic opal in the samples, and solution absorbance after the reaction was obtained using an ultraviolet spectrophotometer. The opal content was calculated by regression equation and the error was less than 3%.

Calcium carbonate content was measured by the method of volume of carbon dioxide using a NFP18-508 Carbonate Analyser. Five hundred milligram of samples were dissolved by excessive hydrochloric acid, and after complete reaction all carbon dioxide was selected. The content of the calcium carbonate was calculated according to standard formula curves. Errors were less than 3%.

Each sample was ground through a 200-μm mesh and then dissolved by the mixture of hydrofluoric acid, perchloric acid and nitric acid; 2% of nitric acid solution was used to dilute the reacted liquid to certain concentrations for instrumental analysis. Ti and RSEs such as Ni, V, and U were measured by ICP-AES and ICP-MS, respectively, with the RSDs less than 5% and 10%.

Four samples were selected for measurement of ^{14}C of organic carbon using accelerator mass spectrometry (AMS). This analysis was completed at the Beta Analytics Laboratory, Miami, United States. The upper limit for age dating of ^{14}C is 43 500 a.

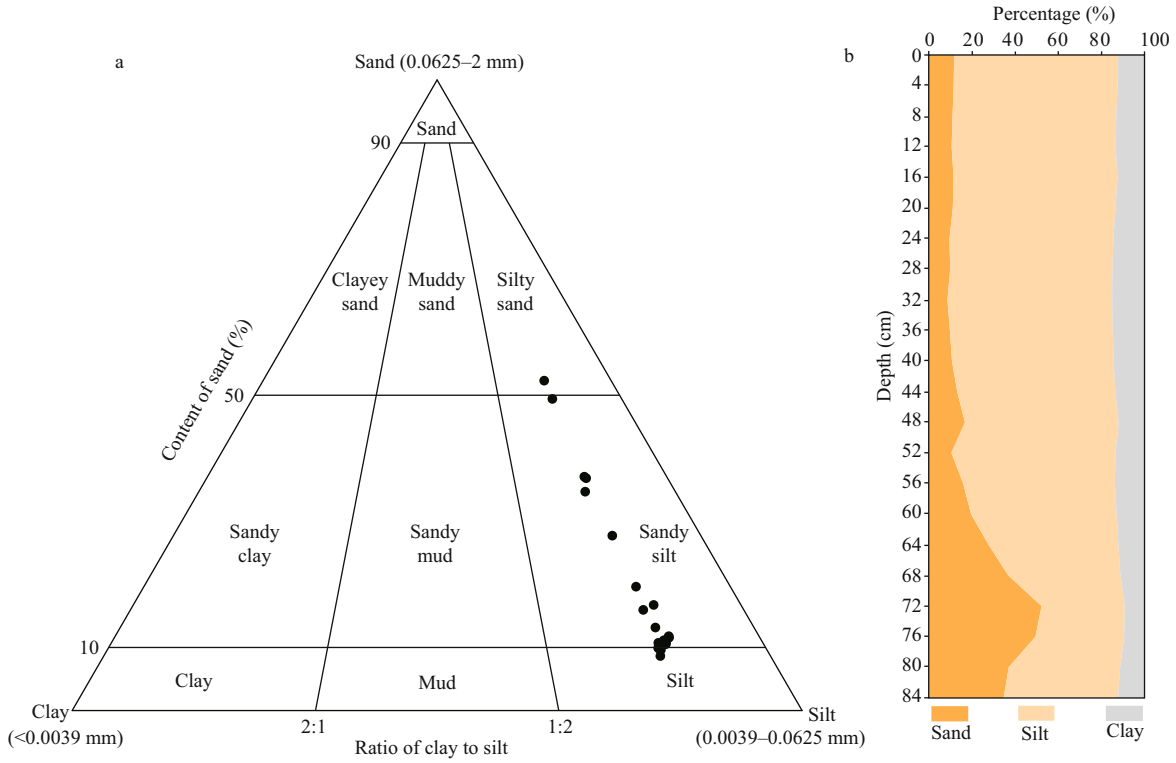

Fig.2 Sediment classification (a) and the proportion of sand, silt and clay (b)

3 RESULT

Biogenic components are summarized and listed in Table 1. The content of TOC ranged from 0.22% to 1.26%, with the mean of 0.90%. The content of TN varied between 0.04% and 0.15%, and the average was 0.11%. Calcium carbonate was only detected in six bottom samples, with the mean of 0.90%. The content of opal was the highest among the biogenic components, ranging from 3.10% to 27.76%, with an average of 20.37%. The lithogenic matter content was calculated according to the following formula (Kawahata et al., 1998): Lithogenic matter %=100%–$CaCO_3$%–Opal%–1.8×TOC%. The lithogenic matter content was between 69.99% and 95.68%, with the mean of 77.75%, indicating that terrigenous materials were dominant in the sediment composition of the Ross Sea. Chondrite-normalized rare earth element (REE) partitioning patterns of Core R11 exhibited the characteristics of relative enrichment of light rare earth element (LREE), the uniform content of heavy rare earth element (HREE), the clear fractionations of LREE and HREE, and the negative anomaly of Eu, denoting that the sediments are mainly derived from the weathering products of the upper continental crust (Fig.3). Apart from terrestrial materials, opal replaced calcium carbonate as the major biogenic component at the core site in the Ross Sea. Previous studies show

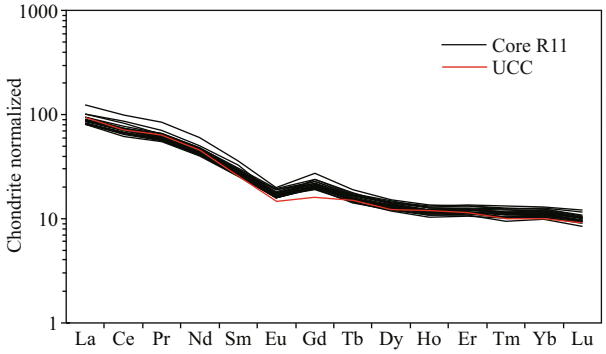

Fig.3 Comparison of REE patterns between Core R11 and UCC

UCC: upper continental crust (Rudnick and Gao, 2003); REE values of Core R11 are from Xiu et al. (2017); Chondrite values are from Haskin et al. (1966).

that diatoms were the dominant taxa, reflecting high marine productivity in Antarctic coastal waters (Bathmann et al., 1997), which accounted for about 75% of primary productivity (Nelson et al., 1995).

There was a significant positive correlation between TOC and TN (Spearman's correlation coefficient =0.857). TOC and opal were also correlated (Spearman's correlation coefficient =0.861). It can be inferred that the production of organic matter in sediments was related to diatom production, and primary productivity of diatoms controlled the absorption and release of carbon by biological pump.

Table 1 Results of multiple components of Core R11

Depth (cm)	Calendar age (cal ka BP)	TOC (%)	TN (%)	$CaCO_3$ (%)	Opal (%)	Lithogenic matter (%)	TOC/TN	Ni/Ti	V/Ti	U/Ti
0	0	1.05	0.15	N/D [c]	26.85	71.25	7.22	76.42	236.90	16.64
4	0.74	1.12	0.14	N/D	26.67	71.31	8.27	85.13	254.23	32.18
8	1.48 [d]	1.24	0.14	N/D	27.76	69.99	8.66	78.90	241.99	19.52
12	2.09	1.26	0.15	N/D	24.20	73.53	8.26	73.96	243.99	16.76
16	2.71	1.16	0.15	N/D	26.04	71.88	7.85	75.81	244.70	20.58
20	3.33	1.25	0.15	N/D	26.32	71.42	8.44	82.47	262.19	21.41
24	3.94	1.16	0.14	N/D	26.21	71.70	8.17	85.31	254.71	19.76
28	4.56 [d]	1.20	0.14	N/D	26.74	71.10	8.66	86.38	268.22	21.40
32	4.63	1.18	0.14	N/D	27.20	70.69	8.36	91.88	277.20	19.36
36	4.71	1.05	0.09	N/D	23.08	75.02	11.69	78.42	257.41	16.19
40	4.78	1.11	0.11	N/D	26.92	71.09	10.07	81.49	259.40	15.43
44	4.86	0.91	0.11	N/D	22.84	75.53	7.90	74.72	242.46	13.06
48	4.93 [d]	0.90	0.12	N/D	23.90	74.47	7.29	76.97	260.55	15.63
52	6.15	1.00	0.10	N/D	23.90	74.29	10.46	88.37	280.20	17.04
56	7.36	0.95	0.12	N/D	20.70	77.59	8.20	89.70	270.06	14.98
60	8.58	0.95	0.12	N/D	20.25	78.03	7.65	79.38	263.38	13.62
64	9.80	0.72	0.13	2.03	15.65	81.02	5.52	130.05	246.11	11.85
68	11.01	0.54	0.07	0.30	12.07	86.65	7.54	60.63	199.14	10.09
72	12.23	0.37	0.04	0.46	7.16	91.71	8.37	62.89	200.75	6.74
76	13.45	0.31	0.06	0.67	3.10	95.68	5.56	55.22	177.13	7.15
78	14.06 [d]	N/A [e]	N/A	N/A	N/A	N/A	N/A	N/A	N/A	N/A
80	N/A	0.22	0.07	1.02	4.96	93.62	3.20	56.21	171.50	5.34
84	N/A	0.23	0.05	0.91	5.65	93.04	4.55	54.02	171.43	6.41
Min	/ [f]	0.22	0.04	0.30	3.10	69.99	3.20	54.02	171.43	5.34
Max	/	1.26	0.15	2.03	27.76	95.68	11.69	130.05	280.20	32.18
Mean	/	0.90	0.11	0.90	20.37	77.75	7.81	78.38	240.17	15.51
S.D. [a]	/	0.34	0.03	0.62	8.09	8.36	1.83	15.79	32.97	6.08
C.V. [b]	/	37%	30%	69%	40%	11%	23%	20%	14%	39%

a: S.D. is standard deviation; b: C.V. is coefficient of variation; c: N/D is not detected; d: these ages are the measured AMS ^{14}C ages, remaining ages are interpolated; e: N/A is not analyzed; f: / is nil.

The preservation rate of organic carbon was only 0.3% (Brummer and Van Eijden, 1992), much lower than that of opal, so the opal content could better reflect productivity changes in the Ross Sea.

4 DISCUSSION

4.1 Establishment of the AMS ^{14}C age framework

The content of calcium carbonate was extremely low and no calcium carbonate shells were found. Therefore, acid-insoluble materials in organic carbon were chosen for AMS ^{14}C dating. Because both the sampling position and water depth of Core R11 were similar to the prior work of Huang et al. (2016), 3045 a, the difference between the organic carbon age and the calcium carbonate age, was adopted as the recalcitrant carbon age for correction. Calendar age was obtained using the age calibration curve of SHCall 13 and Calib 7.0.4 software (Hogg et al., 2013). The dating results are listed in Table 2. Linear interpolation and extrapolation were used to calculate the remainder of Core R11.

Table 2 AMS ^{14}C data of Core R11 in the Ross Sea

Depth (cm)	Material	AMS ^{14}C age (a BP)	Calendar range (cal a BP, 1σ)	Calendar age (cal a BP)
8	Organic carbon	4 670±30	1 470–1 517	1 479
28	Organic carbon	7 160±30	4 521–4 579	4 556
48	Organic carbon	7 470±30	4 878–4 942	4 931
78	Organic carbon	15 250±50	14 003–14 103	14 055

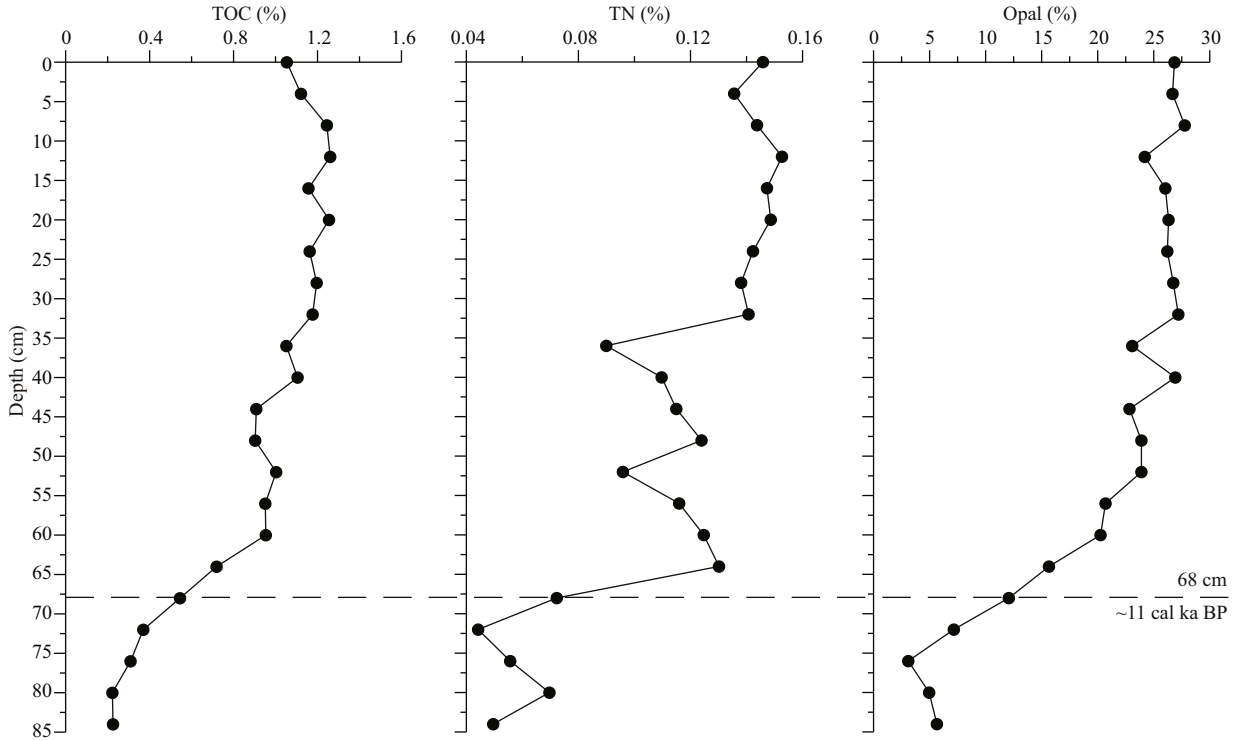

Fig.4 Vertical content variations of biogenic components

4.2 Source of organic matter

The TOC/TN ratio of marine organic matter in sediments is generally from 8 to 9 (Thunell et al., 1992), and that of terrestrial organic matter varies between 20 and 200 (Hedges et al., 1986). Hence, the TOC/TN ratio in this core was an effective index to distinguish the source of organic matter. The TOC/TN ratios of Core R11 ranged from 3.20 to 11.69, most ratios being below 9. This indicates that organic matter was produced by marine phytoplankton, and that organic carbon was controlled by the biological pump. Elemental silicon controls the ocean carbon cycle by affecting the growth of siliceous organisms (Tréguer, 2002). The significant positive correlation between TOC and opal showed that the source of organic matter in the Ross Sea had strong connections with the production of diatoms. Diatoms, as a key sea ice associated organism in the Southern Ocean, are representative of marine primary productivity, and facilitate the transport of organic matter and siliceous shells to the seabed (Nelson et al., 1995; Bathmann et al., 1997).

4.3 Indication for change of marine productivity

Figure 4 shows that the contents of biogenic components decreased with depth in the core overall, but changed more significantly at the core depth of 68 cm, which corresponds to the calendar age of 11 ka BP. The contents of TOC, TN and opal at the core depth of 68–84 cm were lower, with an average of 0.33%, 0.06% and 6.59%, respectively. However, those percentages increased to 1.07%, 0.13% and 24.43%, respectively, in the middle and upper core segments above 68 cm. The vertical variations of the biogenic components can be interpreted as an upward shift in marine productivity since 11 cal ka BP.

The numerical ice sheet model of Golledge et al. (2014) represented very fast mass loss rate of at 11.6–10.2 cal ka BP. The content of ice rafted debris of Core JB06 in the Ross Sea reached a peak at 11.7–5 cal ka BP (Huang et al., 2016). These all indicated that a rapid retreat of ice shelf occurred in the early Holocene. This retreat should be related to the Antarctica early Holocene optimum, which was also recorded in the marine sediments in Antarctic ice cores and Atlantic and Pacific sectors of the Southern Ocean (Masson et al., 2000; Bostock et al., 2013; Xiao et al., 2016). The increase of temperature and southward moving of Circumpolar Deep Water upwelling were considered to promoted the melting of ice shelf (Xiao et al., 2016). Studies had shown that the flourishing of marine phytoplankton dominated by diatoms often occurred at the edge of melting sea ice (DeMaster et al., 1992; Rella et al., 2012). The biogenic components of Core R11 revealed an

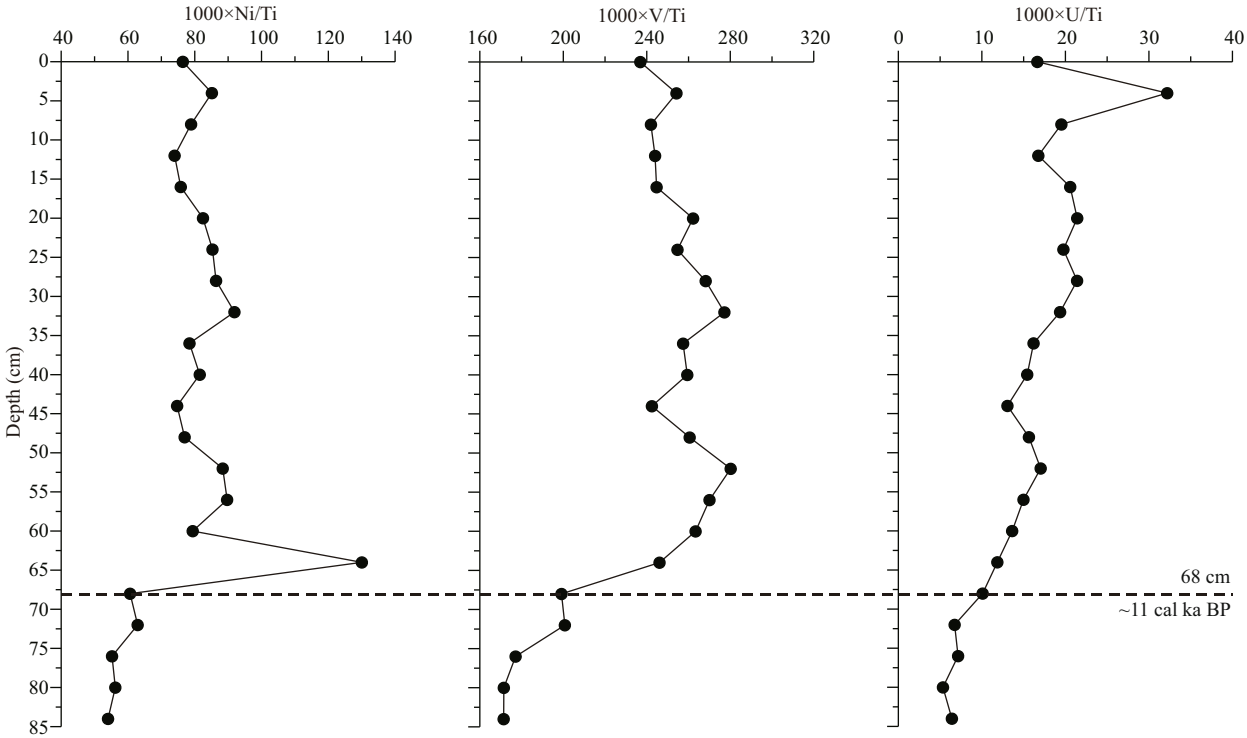

Fig.5 Vertical variations of RSE/Ti ratios of Core R11

obvious shift in marine productivity at ~11 cal ka BP, which was inferred to be related to the ice shelf retreat. The environment possibly changed from non-open marine to open marine in the last deglaciation. But more evidences and further studies were needed.

4.4 Change of sedimentary environment

In Core R11, the foraminfera *Miliammina arenacea* was only found in sediments above the depth of 68 cm, and at the bottom were some other species of calcareous foraminifera (details to be presented elsewhere). *M. arenacea* has strong adaptability to low temperatures and corrosive water conditions (Ishman and Sperling, 2002; Majewski and Anderson, 2009), and its presence indicates property changes of Ross Sea bottom water at the time the sediment layer at 68 cm was deposited, corresponding to ~11 cal ka BP. Two possibilities for the formation of these calcium-dissolving waters include sedimentary depths under the carbonate compensation depth (CCD); or that high productivity in the euphotic zone after ~11 cal ka BP resulted in organic carbon dissolution closer to the seafloor, leading to more corrosive waters. The water depth of sampling position however was 448 m, far above the CCD in the Southern Ocean, and besides, there were diatom and radiolarian tests in the middle and upper portions of the core addition to *M. arenacea*. Therefore, it was inferred that the second possibility was much more likely and the high productivity in the upper water body was related to the retrogression of the ice shelf, opening up open water for production.

RSEs exhibited distinctive occurrences at different oxidation-reduction intervals, which reflect changes in the oxygen concentration in bottom waters and at the water-sediment interface (Calvert and Pedersen, 1993; Tribovillard, et al., 2006). For example, Ni, V and U, can be used to study the redox environment because they were enriched in anoxic marine sediments and have lower concentrations in oxidizing marine sediments. Ti was used to standardize RSEs concentrations to normalize granularity effects and dilution on terrigenous cuttings from biogenic materials.

Similarly, from the core depth of 68 cm downward, the RSE/Ti values were relatively low (Fig.5), while those above core depth of 68 cm significantly increased, revealing that the sedimentary environment had changed at that time. Spearman's correlation coefficients of opal vs Ni/Ti, opal vs V/Ti, and opal vs U/Ti are 0.483, 0.495, and 0.892, respectively. The RSE/Ti value was positively correlated with opal content, indicating that the change of redox environment was related to that of productivity. The marine productivity at the core depth of 68–84 cm was relatively low, thus the flux of organic matter sinking to the seafloor was low, too. Oxygen in the

bottom water was likely higher due to lower respiration rates for organic matter (Galbraith and Jaccard, 2015). The enough oxygen in the bottom water body led to the reduction of RSEs contents. From the core depth of 68 cm upwards, marine productivity increased, based upon the increase in organic matter reaching the seabed. The decomposition of additional organic matter would have consumed oxygen, causing a rapid decline in dissolved oxygen at the sediment-water interface. The RSEs contents in the sediment subsequently rose due to the apparent decline in dissolved oxygen. Simultaneously, more carbon dioxide was produced during the decomposition of organic matter and making bottom waters more corrosive to calcium carbonate. It should be noted that the contents of Ni, V and U in Core R11 were generally low, indicating that the sedimentary environment was never anoxic (Morford and Emerson, 1999; Tribovillard et al., 2006; Wang et al., 2018). This work is consistent with previous research that has showed that fluctuations in dissolved oxygen content in the bottom waters of the Ross Sea since the late Quaternary, with no anoxic events (Ceccaroni et al., 1998).

5 CONCLUSION

Opal was the major biogenic component in the sediments of the Ross Sea and had a significant positive correlation with TOC, which indicated that silicon producing phytoplankton, were the main producers of marine organic matter.

The contents of biogenic components in the bottom portion of the core (at depth of 68–84 cm) and in the middle and upper part (at the core depth of 0–68 cm) were distinct, revealing that marine productivity changed abruptly at ~11 cal ka BP. This change was primarily related to the melting and retrogression of the Ross Ice Shelf, opening up open water for production.

The sedimentary environment revealed by foraminifera fossils and RSE/Ti ratios also changed at ~11 cal ka BP. The promotion of marine productivity since ~11 cal ka BP led to more organic matter reaching the seabed. The decomposition of this organic matter has lowered dissolved oxygen in the bottom waters, resulting in the rapid decreases of dissolved oxygen at the sediment-water interface.

6 DATA AVAILABILITY STATEMENT

The data generated during and/or analyzed during the current study are available from the corresponding author on reasonable request.

7 ACKNOWLEDGMENT

We thank the Chinese National Antarctic Research Expedition for the sampling effort.

References

Anderson J B, Conway H, Bart P J, Witus A E, Greenwood S L, McKay R M, Hall B L, Ackert R P, Licht K, Jakobsson M, Stone J O. 2014. Ross Sea paleo-ice sheet drainage and deglacial history during and since the LGM. *Quaternary Science Reviews*, **100**: 31-54, https://doi.org/10.1016/j.quascirev.2013.08.020.

Barnola J M, Raynaud D, Korotkevich Y S, Lorius C. 1987. Vostok ice core provides 160,000-year record of atmospheric CO_2. *Nature*, **329**(6138): 408-414, https://doi.org/10.1038/329408a0.

Bathmann U V, Scharek R, Klaas C, Dubischar C D, Smetacek V. 1997. Spring development of phytoplankton biomass and composition in major water masses of the Atlantic sector of the Southern Ocean. *Deep Sea Research Part II*: *Topical Studies in Oceanography*, **44**(1-2): 51-67, https://doi.org/10.1016/S0967-0645(96)00063-X.

Bentaleb I, Fontugne M. 1998. The role of the southern Indian Ocean in the glacial to interglacial atmospheric CO_2 change: organic carbon isotope evidences. *Global and Planetary Change*, **16-17**: 25-36, https://doi.org/10.1016/S0921-8181(98)00004-6.

Bonn W J, Gingele F X, Grobe H, Mackensen A, Fütterer D K. 1998. Palaeoproductivity at the Antarctic continental margin: opal and barium records for the last 400 ka. *Palaeogeography*, *Palaeoclimatology*, *Palaeoecology*, **139**(3-4): 195-211, https://doi.org/10.1016/S0031-0182(97)00144-2.

Bostock H C, Barrows T T, Carter L, Chase Z, Cortese G, Dunbar G B, Ellwood M, Hayward B, Howard W, Neil H L, Noble T L, Mackintosh A, Moss P T, Moy A D, White D, Williams M J M, Armand L K. 2013. A review of the Australian-New Zealand sector of the Southern Ocean over the last 30 ka (Aus-INTIMATE project). *Quaternary Science Reviews*, **74**: 35-57, https://doi.org/10.1016/j.quascirev.2012.07.018.

Brummer G J A, Van Eijden A J M. 1992. "Blue-ocean" paleoproductivity estimates from pelagic carbonate mass accumulation rates. *Marine Micropaleontology*, **19**(1-2): 99-117, https://doi.org/10.1016/0377-8398(92)90023-D.

Calvert S E, Pedersen T F. 1993. Geochemistry of recent oxic and anoxic marine sediments: implications for the geological record. *Marine Geology*, **113**(1-2): 67-88, https://doi.org/10.1016/0025-3227(93)90150-T.

Ceccaroni L, Frank M, Frignani M, Langone L, Ravaioli M, Mangini A. 1998. Late Quaternary fluctuations of biogenic component fluxes on the continental slope of the Ross Sea, Antarctica. *Journal of Marine Systems*, **17**(1-4): 515-

525, https://doi.org/10.1016/S0924-7963(98)00061-X.

Davey F J, Bennett D J, Houtz R E. 1982. Sedimentary basins of the Ross Sea, Antarctica. *New Zealand Journal of Geology and Geophysics*, **25**(2): 245-255, https://doi.org/10.1080/00288306.1982.10421413.

DeMaster D J, Dunbar R B, Gordon L I, Leventer A R, Morrison J M, Nelson D M, Nittrouer C A, Smith Jr W O. 1992. Cycling and accumulation of biogenic silica and organic matter in high-latitude environments: the Ross Sea. *Oceanography*, **5**(3): 146-153, https://doi.org/10.5670/oceanog.1992.03.

Fagel N, Dehairs F, André L, Bareille G, Monnin C. 2002. Ba distribution in surface Southern Ocean sediments and export production estimates. *Paleoceanography*, **17**(2): 1011, https://doi.org/10.1029/2000PA000552.

Folk R L, Andrews P B, Lewis D W. 1970. Detrital sedimentary rock classification and nomenclature for use in New Zealand. *New Zealand Journal of Geology and Geophysics*, **13**(4): 937-968, https://doi.org/10.1080/00288306.1970.10418211.

Galbraith E D, Jaccard S L. 2015. Deglacial weakening of the oceanic soft tissue pump: global constraints from sedimentary nitrogen isotopes and oxygenation proxies. *Quaternary Science Reviews*, **109**: 38-48, https://doi.org/10.1016/j.quascirev.2014.11.012.

Gao Z Y, Chen L Q, Wang W Q. 2001. Air-sea fluxes and the distribution of sink and source of CO_2 between 80°W and 80°E in the Southern Ocean. *Chinese Journal of Polar Research*, **13**(3): 175-186. (in Chinese with English abstract)

Golledge N R, Menviel L, Carter L, Fogwill C J, England M H, Cortese G, Levy R H. 2014. Antarctic contribution to meltwater pulse 1A from reduced Southern Ocean overturning. *Nature Communications*, **5**: 5 107, https://doi.org/10.1038/ncomms6107.

Graham R M, De Boer A M, Van Sebille E, Kohfeld K E, Schlosser C. 2015. Inferring source regions and supply mechanisms of iron in the Southern Ocean from satellite chlorophyll data. *Deep Sea Research Part I*: *Oceanographic Research Papers*, **104**: 9-25, https://doi.org/10.1016/j.dsr.2015.05.007.

Haskin L A, Frey F A, Schmitt R A, Smith R H. 1966. Meteoritic, solar and terrestrial rare-earth distributions. *Physics and Chemistry of the Earth*, **7**: 167-321, https://doi.org/10.1016/0079-1946(66)90004-8.

Hedges J I, Clark W A, Quay P D, Richey J E, Devol A H, Santos M. 1986. Compositions and fluxes of particulate organic material in the Amazon River. *Limnology and Oceanography*, **31**(4): 717-738, https://doi.org/10.4319/lo.1986.31.4.0717.

Hiscock M R, Marra J, Smith Jr W O, Goericke R, Measures C, Vink S, Olson R J, Sosik H M, Barber R T. 2003. Primary productivity and its regulation in the Pacific Sector of the Southern Ocean. *Deep Sea Research Part II*: *Topical Studies in Oceanography*, **50**(3-4): 533-558, https://doi.org/10.1016/S0967-0645(02)00583-0.

Hogg A G, Hua Q, Blackwell P G, Biu M, Buck C E, Guilderson T P, Heaton T J, Palmer J G, Reimer P J, Reimer R W, Turney C S M, Zimmerman S R H. 2013. SHCal13 Southern Hemisphere calibration, 0-50,000 years cal BP. *Radiocarbon*, **55**(4): 1 889-1 903, https://doi.org/10.2458/azu_js_rc.55.16783.

Hu C Y, Yao M, Yu P S, Pan J M, Zhang H S. 2007. Biogenic silica in surficial sediments of Prydz Bay of the Southern Ocean. *Acta Oceanologica Sinica*, **29**(5): 48-54, https://doi.org/10.3321/j.issn:0253-4193.2007.05.006. (in Chinese with English abstract)

Huang M X, Wang R J, Xiao W S, Wu L, Chen Z H. 2016. Retreat process of Ross Ice Shelf and hydrodynamic changes on northwestern Ross continental shelf since the last glacial. *Marine Geology & Quaternary Geology*, **36**(5): 97-108, https://doi.org/10.16562/j.cnki.0256-1492.2016.05.010. (in Chinese with English abstract)

Ishman S E, Sperling M R. 2002. Benthic foraminiferal record of Holocene deep-water evolution in the Palmer Deep, western Antarctic Peninsula. *Geology*, **30**(5): 435-438, https://doi.org/10.1130/0091-7613(2002)030<0435:BFROHD>2.0.CO;2.

Kawahata H, Suzuki A, Ahagon N. 1998. Biogenic sediments in the West Caroline Basin, the western equatorial Pacific during the last 330,000 years. *Marine Geology*, **149**(1-4): 155-176, https://doi.org/10.1016/S0025-3227(98)00039-5.

Li L, Wang H, Luo B R C, He J. 2008. The characterizations and paleoceanographic significances of organic and inorganic carbon in northern South China Sea during past 40 ka. *Marine Geology & Quaternary Geology*, **28**(6): 79-85. (in Chinese with English abstract)

Lin H L, Lai C T, Ting H C, Wang L J, Sarnthein M, Hung J J. 1999. Late Pleistocene nutrients and sea surface productivity in the South China Sea: a record of teleconnections with Northern hemisphere events. *Marine Geology*, **156**(1-4): 197-210, https://doi.org/10.1016/S0025-3227(98)00179-0.

Liu S F, Shi X F, Liu Y G, Zhai B, Wu Y H. 2011. High-resolution record of biogenic silica and its paleoproductivity implication in mud area, East China Sea inner shelf over the last 2000 years BP. *Acta Sedimentologica Sinica*, **29**(2): 321-327. (in Chinese with English abstract)

Majewski W, Anderson J B. 2009. Holocene foraminiferal assemblages from Firth of Tay, Antarctic Peninsula: paleoclimate implications. *Marine Micropaleontology*, **73**(3-4): 135-147, https://doi.org/10.1016/j.marmicro.2009.08.003.

Masson V, Vimeux F, Jouzel J, Morgan M, Ciais P, Hammer C, Johnsen S, Lipenkov V Y, Mosley-Thompson E, Petit J R, Steig E J, Stievenard M, Vaikmae R. 2000. Holocene climate variability in Antarctica based on 11 ice-core isotopic records. *Quaternary Research*, **54**(3): 348-358, https://doi.org/10.1006/qres.2000.2172.

Morford J L, Emerson S. 1999. The geochemistry of redox sensitive trace metals in sediments. *Geochimica et Cosmochimica Acta*, **63**(11-12): 1 735-1 750, https://doi.org/10.1016/S0016-7037(99)00126-X.

Nelson D M, Tréguer P, Brzezinski M A, Leynaert A, Quéguiner B. 1995. Production and dissolution of biogenic silica in the ocean: revised global estimates, comparison with regional data and relationship to biogenic sedimentation. *Global Biogeochemical Cycles*, **9**(3): 359-372, https://doi.org/10.1029/95GB01070.

Paytan A, Kastner M, Chavez F P. 1996. Glacial to interglacial fluctuations in productivity in the equatorial Pacific as indicated by marine barite. *Science*, **274**(5291): 1 355-1 357, https://doi.org/10.1126/science.274.5291.1355.

Raynaud D, Barnola J M, Chappellaz J, Zardini D, Jouzel J, Lorius C. 1992. Glacial-interglacial evolution of greenhouse gases as inferred from ice core analysis: a review of recent results. *Quaternary Science Reviews*, **11**(4): 381-386, https://doi.org/10.1016/0277-3791(92)90020-9.

Rella S F, Tada R, Nagashima K, Ikehara M, Itaki T, Ohkushi K, Sakamoto T, Harada N, Uchida M. 2012. Abrupt changes of intermediate water properties on the northeastern slope of the Bering Sea during the last glacial and deglacial period. *Paleoceanography*, **27**(3): PA3203, https://doi.org/10.1029/2011PA002205.

Rudnick R L, Gao S. 2003. Composition of the continental crust. Treatise on Geochemistry, **3**: 1-64.

Ship S, Anderson J, Domack E. 1999. Late Pleistocene-Holocene retreat of the West Antarctic Ice-Sheet system in the Ross Sea: part 1—geophysical results. *GSA Bulletin*, **111**(10): 1 486-1 516, https://doi.org/10.1130/0016-7606(1999)111<1486:LPHROT>2.3.CO;2.

Tan S Z, Yu P S, Hu C Y, Han Z B, Zhang H S. 2014. Biogenic barium in surface sediments of Prydz Bay, Antarctica. *Chinese Journal of Polar Research*, **26**(3): 300-305, https://doi.org/10.13679/j.jdyj.2014.3.300. (in Chinese with English abstract)

Thunell R C, Miao Q M, Calvert S E, Pedersen T F. 1992. Glacial-Holocene biogenic sedimentation patterns in the South China Sea: productivity variations and surface water pCO_2. *Paleoceanography*, **7**(2): 143-162, https://doi.org/10.1029/92PA00278.

Tréguer P. 2002. Silica and the cycle of carbon in the ocean. *Comptes Rendus Geoscience*, **334**(1): 3-11, https://doi.org/10.1016/S1631-0713(02)01680-2.

Tribovillard N, Algeo T J, Lyons T, Riboulleau A. 2006. Trace metals as paleoredox and paleoproductivity proxies: an update. *Chemical Geology*, **232**(1-2): 12-32, https://doi.org/10.1016/j.chemgeo.2006.02.012.

Wang J K, Li T G, Xiong Z F, Chang F M, Qin B B, Wang L Y, Jia Q. 2018. Sedimentary gochemical characteristics of the redox-sensitive elements in Ross Sea, Antarctica: implications for paleoceanography. *Marine Geology & Quaternary Geology*, **38**(5): 112-121, https://doi.org/10.16562/j.cnki.0256-1492.2018.05.011. (in Chinese with English abstract)

Xiao W S, Esper O, Gersonde R. 2016. Last Glacial-Holocene climate variability in the Atlantic sector of the Southern Ocean. *Quaternary Science Reviews*, **135**: 115-137, https://doi.org/10.1016/j.quascirev.2016.01.023.

Xiu C, Chen X X, Zhou M J, Xu M N, Zhang X, Xing J. 2017. REE geochemical characteristics of Core R11 in the Ross Sea, Antarctic. *Marine Geology Frontiers*, **33**(5): 1-8, https://doi.org/10.16028/j.1009-2722.2017.05001. (in Chinese with English abstract)